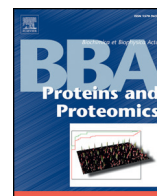




Contents lists available at ScienceDirect

Biochimica et Biophysica Acta

journal homepage: www.elsevier.com/locate/bbapap

Effect of Zn^{2+} binding and enzyme active site on the transition state for RNA 2'-O-transphosphorylation interpreted through kinetic isotope effects[☆]

Haoyuan Chen^{a,b}, Joseph A. Piccirilli^c, Michael E. Harris^d, Darrin M. York^{d,*}

^a Center for Integrative Proteomics Research, BioMaPS Institute for Quantitative Biology, Rutgers University, Piscataway, NJ 08854, United States

^b Department of Chemistry and Chemical Biology, Rutgers University, Piscataway, NJ 08854, United States

^c Department of Chemistry, Department of Biochemistry and Molecular Biology, University of Chicago, Chicago, IL 60637, United States

^d Department of Biochemistry, Center for Proteomics and Bioinformatics, Case Western Reserve University School of Medicine, Cleveland, OH 44106, United States

ARTICLE INFO

Article history:

Received 18 November 2014

Received in revised form 26 February 2015

Accepted 27 February 2015

Available online xxx

Keywords:

Kinetic isotope effect

Transition state

Transphosphorylation

Zn^{2+} binding

Enzyme

ABSTRACT

Divalent metal ions, due to their ability to stabilize high concentrations of negative charge, are important for RNA folding and catalysis. Detailed models derived from the structures and kinetics of enzymes and from computational simulations have been developed. However, in most cases the specific catalytic modes involving metal ions and their mechanistic roles and effects on transition state structures remain controversial. Valuable information about the nature of the transition state is provided by measurement of kinetic isotope effects (KIEs). However, KIEs reflect changes in all bond vibrational modes that differ between the ground state and transition state. QM calculations are therefore essential for developing structural models of the transition state and evaluating mechanistic alternatives. Herein, we present computational models for Zn^{2+} binding to RNA 2'-O-transphosphorylation reaction models that aid in the interpretation of KIE experiments. Different Zn^{2+} binding modes produce distinct KIE signatures, and one binding mode involving two zinc ions is in close agreement with KIEs measured for non-enzymatic catalysis by Zn^{2+} aquo ions alone. Interestingly, the KIE signatures in this specific model are also very close to those in RNase A catalysis. These results allow a quantitative connection to be made between experimental KIE measurements and transition state structure and bonding, and provide insight into RNA 2'-O-transphosphorylation reactions catalyzed by metal ions and enzymes. This article is part of a Special Issue entitled: Enzyme Transition States from Theory and Experiment.

© 2015 Published by Elsevier B.V.

1. Introduction

Divalent metal ions play critical roles in RNA folding and catalysis [1–8]. The ability of divalent ions to stabilize high concentrations of negative charge in transphosphorylation reaction centers via electrostatic interactions, direct coordination or acid-base chemistry empowers them with potential mechanisms to assist in catalysis. However, unraveling the specific role of metal ions is extremely challenging due to the difficulty in discerning the catalytically active metal ion binding mode and its connection with the transition state (TS) structure and

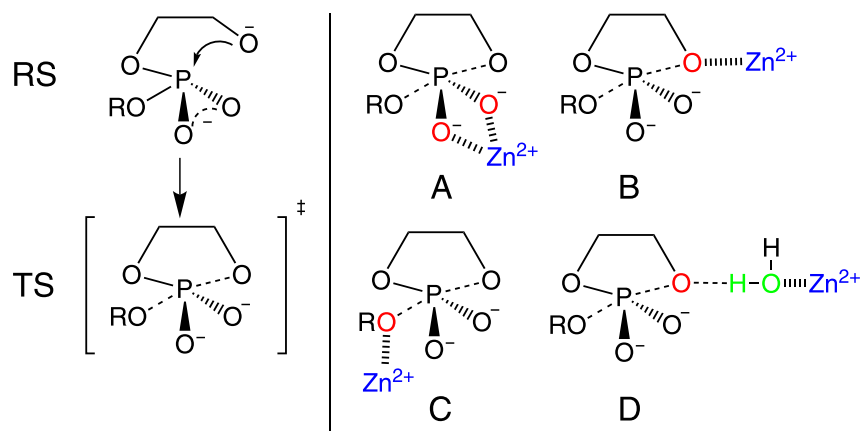
bonding [2–4], which also exists as the major barrier in the investigation of enzyme catalysis mechanisms.

A powerful strategy to resolve mechanistic ambiguity is to rationally design and study simplified model reaction systems using a joint experimental/theoretical approach. Perhaps the most sensitive experimental mechanistic probe is the measurement of kinetic isotope effects (KIEs) that compare the relative reaction rate constants between isotopologues. KIEs arise from subtle quantum effects associated with the changes in structure and bonding that occur in proceeding from the reactant state (RS) to rate-controlling TS [9–14]. However, meaningful interpretation of KIE measurements requires the use of computational models. Computational modeling of KIEs has been extensively applied to study RNA transphosphorylation catalyzed by enzyme, [15] specifically designed metal catalyst [16,17] and without catalyst [18–20]. In a recent work, [21] Zhang et al. measured the primary and secondary kinetic isotope effects for catalysis by Zn^{2+} ions and by

[☆] This article is part of a Special Issue entitled: Enzyme Transition States from Theory and Experiment.

* Corresponding author.

E-mail address: york@biomaps.rutgers.edu (D.M. York).



Scheme 1. (Left) Schematic description of the reactant state and rate-limiting transition state in the RNA transphosphorylation reaction model. (Right) Illustration of three different Zn^{2+} binding sites (non-bridging oxygens in A, nucleophile oxygen in B, leaving group oxygen in C) and two interaction modes (direct coordination in A, B and C, indirect binding via a solvent water molecule in D).

specific base alone, and compared results with preliminary calculations. In the present work, we extend the scope of these calculations to explore 9 distinct, alternative Zn^{2+} ion binding modes (Fig. 2) within several classes (Scheme 1) in the TS and characterize the resulting KIE signatures. Comparison across different model reactions is also performed and analyzed.

2. Results and discussion

2.1. Building a baseline model for un-catalyzed RNA 2'-O-transphosphorylation

In order to understand the effect of Zn^{2+} binding on TS structure, it is necessary to first characterize the reaction mechanism and TS in the absence of Zn^{2+} . The transition states for a series of non-enzymatic baseline models (B1–B3) in the absence of Zn^{2+} are shown in Fig. 1, and their calculated KIEs are compared with experimental values [15] for a UpG dinucleotide in Table 1. As the models progress from the minimal model (B1) to the full dinucleotide (B3), the agreement between the calculated and experimental $^{18}k_{\text{LG}}$ values significantly improves, while for $^{18}k_{\text{NUC}}$ and $^{18}k_{\text{NPO}}$ it improves slightly in B3 but not B2. The notable decrease in the calculated $^{18}k_{\text{LG}}$ value from 1.0416 in B1 to

1.0358 in B2 mainly arises from the addition of a sugar ring to the leaving group, which enhances the leaving group activity since the $\text{p}K_{\text{a}}$ of tetrahydro-2-furanmethanol (14.68 [22]) is lower than that of ethanol (16.47 [22]). The addition of the full guanosine leaving group (B3) further reduces the $^{18}k_{\text{LG}}$ value to 1.0322 that is very close to the experimental value of 1.034. This is due to coupling of vibrational modes of the nucleobase, in addition to the overall greater effective mass of the leaving group that damps the frequency of certain key modes. It is noteworthy to mention that when the leaving group is a methoxide, which is even lighter than the ethoxide group of B1, the calculated $^{18}k_{\text{LG}}$ value increases to 1.0649, despite having a $\text{p}K_{\text{a}}$ value roughly 0.5 units lower [20].

Although the full dinucleotide baseline model (B3) is in best agreement with experiment, it is too computationally intensive to be practical as a departure point from which to exhaustively explore multiple Zn^{2+} binding modes that add many more electrons to the quantum system and degrees of freedom to the optimization procedure. The goal of the present work is to determine the effect of Zn^{2+} binding on the TS structure of the UpG dinucleotide. As seen in Table 1, while the absolute values of the calculated KIEs for catalyzed and uncatalyzed reactions deviate modestly from the experimental values, their relative values

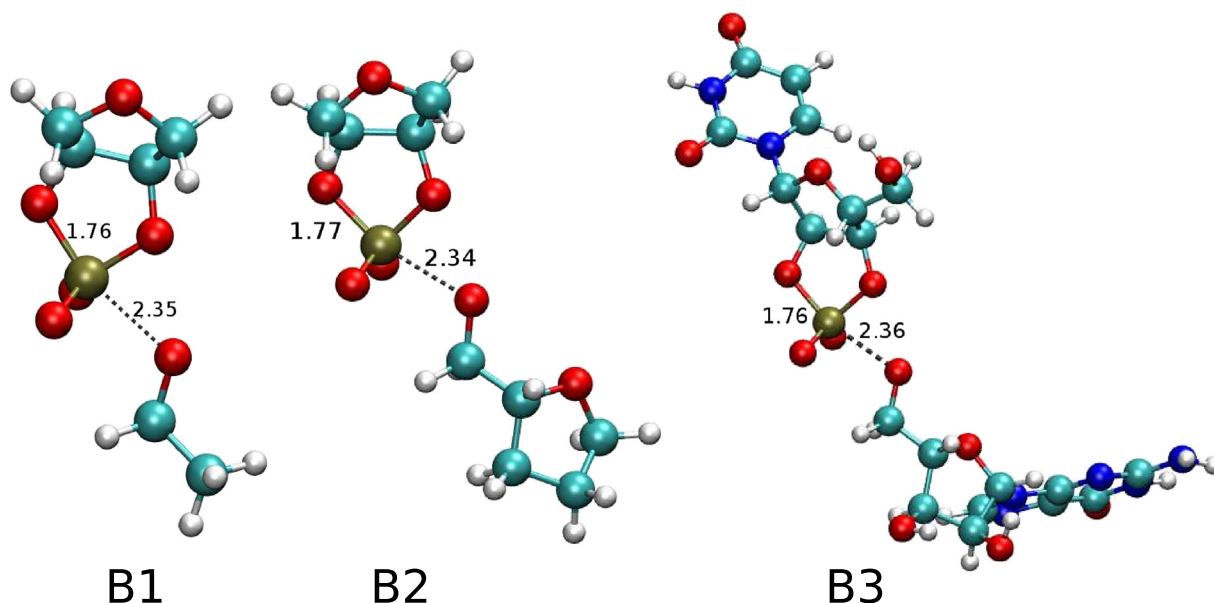


Fig. 1. TS structures of baseline models for un-catalyzed RNA transphosphorylation. Key bond lengths in Å are labeled.

Table 1

Comparison of calculated and experimental KIE values and the effect of catalysts for UpG dinucleotide 2'-O transphosphorylation model reactions in solution.

Condition	$^{18}k_{LG}$	$^{18}k_{NUC}$	$^{18}k_{NPO}$
Model B1 calc.	1.0416	1.0016	1.0029
Model B2 calc.	1.0358	1.0038	1.0032
Model B3 calc.	1.0322	1.0011	1.0025
Baseline expt. [18]	1.034(3)	0.997(1)	0.999(1)
Zn model IX calc.	1.0276	0.9950	1.0028
Zn ²⁺ -catalyzed expt. [21]	1.015(2)	0.986(4)	1.0007(2)
$(k^{cat}/k^{BL})_{Calc.}$	0.986	0.993	1.000
$(k^{cat}/k^{BL})_{Expt.}$	0.982	0.989	1.002
RNase A calc. [20]	1.0272	0.9973	1.0060
RNase A expt. [15]	1.014(3)	0.994(2)	1.001(1)
$(k^{cat}/k^{BL})_{Calc.}$	0.986	0.996	1.003
$(k^{cat}/k^{BL})_{Expt.}$	0.981	0.997	1.002

All KIE values were measured/calculated at the temperature of 90 °C except for $^{18}k_{NPO}$ in the baseline models, where the only available experimental value was at 37 °C (from Ref. 18). Therefore, the corresponding calculations were also performed at 37 °C. k^{cat}/k^{BL} quantifies the effect of the catalyst on the KIEs, which is the ratio between KIEs in the catalyzed and uncatalyzed reactions, where the BL refers to the baseline model B1.

are very consistent. Our comparison focuses on the relative KIEs for the catalyzed and uncatalyzed (baseline) models in order to maximize the cancellation of systematic errors in order to obtain *quantitative agreement* of the relative calculated and experimental KIE values. It has been suggested [23] to use isotope-effect-minus-one (KIE – 1) instead of KIE itself when comparing heavy atom isotope effects as these values are usually very close to unity. Here since we're focusing on the ratio between catalyzed and un-catalyzed KIEs, subtracting by one will make the magnitudes of both numerator and denominator much smaller, which will make the result a lot more sensitive to the computational errors and experimental uncertainties because both numerator and denominator are now in similar orders of magnitude with the uncertainties. It might also blow up because the denominator could be very close to zero. With an understanding of the deviations of the minimal baseline model (B1) relative to the dinucleotide baseline model (B3), it is reasonable to expect that comparison of Zn²⁺ binding in the context of the minimal model (which is computationally tractable even with multiple hydrated Zn²⁺ ions bound) would be transferable to the dinucleotide. Consequently, in what follows, we use the minimal baseline model (B1) as a framework from which to calculate the effect of Zn²⁺ binding on the TS and KIE values.

2.2. Exploration of Zn²⁺ catalytic modes

Comparison of experimental KIEs for un-catalyzed (baseline) and Zn²⁺-catalyzed reactions (Table 1) indicate that both primary $^{18}k_{LG}$ and $^{18}k_{NUC}$ values decrease considerably (by 0.019 and 0.011) upon Zn²⁺ binding. Examination of the experimental ratio of the KIE values for Zn²⁺-catalyzed and baseline reactions [$(k^{cat}/k^{BL})_{Expt.}$] indicates the largest deviation from unity occurs for the leaving group (1.8%). The large normal $^{18}k_{LG}$ value for the uncatalyzed reaction (1.034) suggests a late transition state characterized by a small bond order to the leaving group and high degree of accumulated charge at the O5' position. The significant reduction of the $^{18}k_{LG}$ value upon Zn²⁺ binding (1.015) suggests a TS that is not as late [20], has greater bonding to the leaving group and less charge at the O5' position. The effect of Zn²⁺ binding on the $^{18}k_{NUC}$ value is also significant (1.1%), but less pronounced than for $^{18}k_{LG}$, and indicates a slightly higher degree of bond formation of the nucleophile to phosphorus for the Zn²⁺-bound TS compared to the un-catalyzed reaction. There is little effect of Zn²⁺ binding on the secondary KIE ($^{18}k_{NPO}$) values (0.2%). The overall effect of Zn²⁺ binding is to produce a generally tighter TS bonding environment.

In order to establish a molecular electronic structure model that explains the effect of Zn²⁺ binding on the KIE values relative to the

uncatalyzed reaction, we examined a series of 9 plausible Zn²⁺ binding modes (Fig. 2), the results for which are shown in Table 2. Agreement between calculated and experimentally measured KIE values can be quantified by examination of the percent deviation (%D) in the KIE ratios defined as $\%D = [(k^{cat}/k^{BL})_{Calc.} - (k^{cat}/k^{BL})_{Expt.}] \times 100\%$. Further, the character of the TS can be quantified by a reaction coordinate ξ defined as $\xi = R_2 - R_1$, where R_1 and R_2 are the P–O2' and P–O5' bond lengths, respectively (Table 2). Negative values of ξ indicate an early TS, whereas positive values indicate a late one.

We first explored a series of representative single Zn²⁺ binding modes to ascertain the effects on the predicted KIE values. In models I and II, Zn²⁺ are placed near the non-bridging oxygens to stabilize the negatively-charged phosphorane TS. However, the TSs are too late ($\xi \sim -0.7$ – -0.8 Å, Table 2) and have $^{18}k_{LG}$ values that are considerably larger than the experimental value. The difference between models I and II involves direct versus indirect Zn²⁺ coordination and does not substantially alter the KIE values. For model III and IV in which Zn²⁺ binds directly and indirectly to the nucleophile O2', the $^{18}k_{NUC}$ becomes slightly normal, and the $^{18}k_{LG}$ values remain large. Models V and VI explore direct and indirect Zn²⁺ binding to the leaving group oxygen, which leads to an early TS ($\xi \sim -0.5$ Å) with considerably underestimated $^{18}k_{LG}$ and overestimated $^{18}k_{NUC}$ values. This can be explained by recognizing that this Zn²⁺ binding mode has a similar effect as that of an enhanced leaving group [20] to shift the TS from late to early in character, with limited bond cleavage and charge accumulation at the O5' position.

The inability for the single Zn²⁺ binding models (I–VI) to reproduce the experimental KIEs leads us to explore dimetal Zn²⁺ binding modes. Models VII and VIII explore direct and indirect Zn²⁺ binding, respectively, at both the nucleophile and leaving group positions. Model VII produces a late transition state ($\xi = 0.47$ Å) that is much earlier than models I–IV and has a considerably improved $^{18}k_{LG}$ value (%D = 1.0), but has a normal $^{18}k_{NUC}$ value with greater deviation (%D = 1.5). Model VIII has a similar late transition state ($\xi = 0.48$ Å) to model VII, but has a nucleophile KIE value that is even more normal, and considerably underestimates the leaving group KIE, resulting from a partial proton transfer from a Zn²⁺-coordinated water to leaving group oxygen.

Interestingly, each different Zn²⁺ binding model has a distinct set of predicted KIE values, however, only model IX corresponds closely with what is observed experimentally. Model IX involves one Zn²⁺ making a direct coordination to the leaving group, and another that makes direct coordination to the non-bridge phosphoryl oxygen while maintaining indirect coordination with the nucleophile (Fig. 2). In this model, the dimetal binding mode provides three distinct elements of TS stabilization—leaving group stabilization, negative charge redistribution and potentially assistance in proton transfer. The nucleophile and leaving group KIE deviations are 0.4% and 0.5%, respectively, a reduction in deviation by a factor of 2 with respect to the next smallest deviations in the series of models. The $^{18}k_{NUC}$ value is slightly inverse and the $^{18}k_{LG}$ value normal. Excellent agreement is obtained between calculated and experimental (k^{cat}/k^{BL}) ratios (Table 1) for the leaving group (0.986 and 0.982, respectively) and nucleophile (0.993 and 0.989, respectively). We've also expanded the leaving group in model IX with a sugar ring as in model B2, but the KIE values calculated from corresponding optimized structures are not significantly different from the original model IX ($^{18}k_{LG} = 1.0268$ vs 1.0276, $^{18}k_{NUC} = 0.9963$ vs 0.9950). Therefore we did not attempt to further expand the model to full UpG as in B3, as these are very large calculations that become more difficult to converge with more degrees of freedom. The general effect of Zn²⁺ binding is to create an earlier TS with an overall stiffer bonding environment that leads to a less pronounced normal leaving group KIE and slightly more inverse nucleophile KIE. The very close agreement of this model with recently measured KIE values, in stark contrast to that of a series of 8 other models tested, provides strong evidence that it can be used to provide an experimental interpretation of the TS structure and bonding for Zn²⁺-catalyzed RNA 2'-O-transphosphorylation.

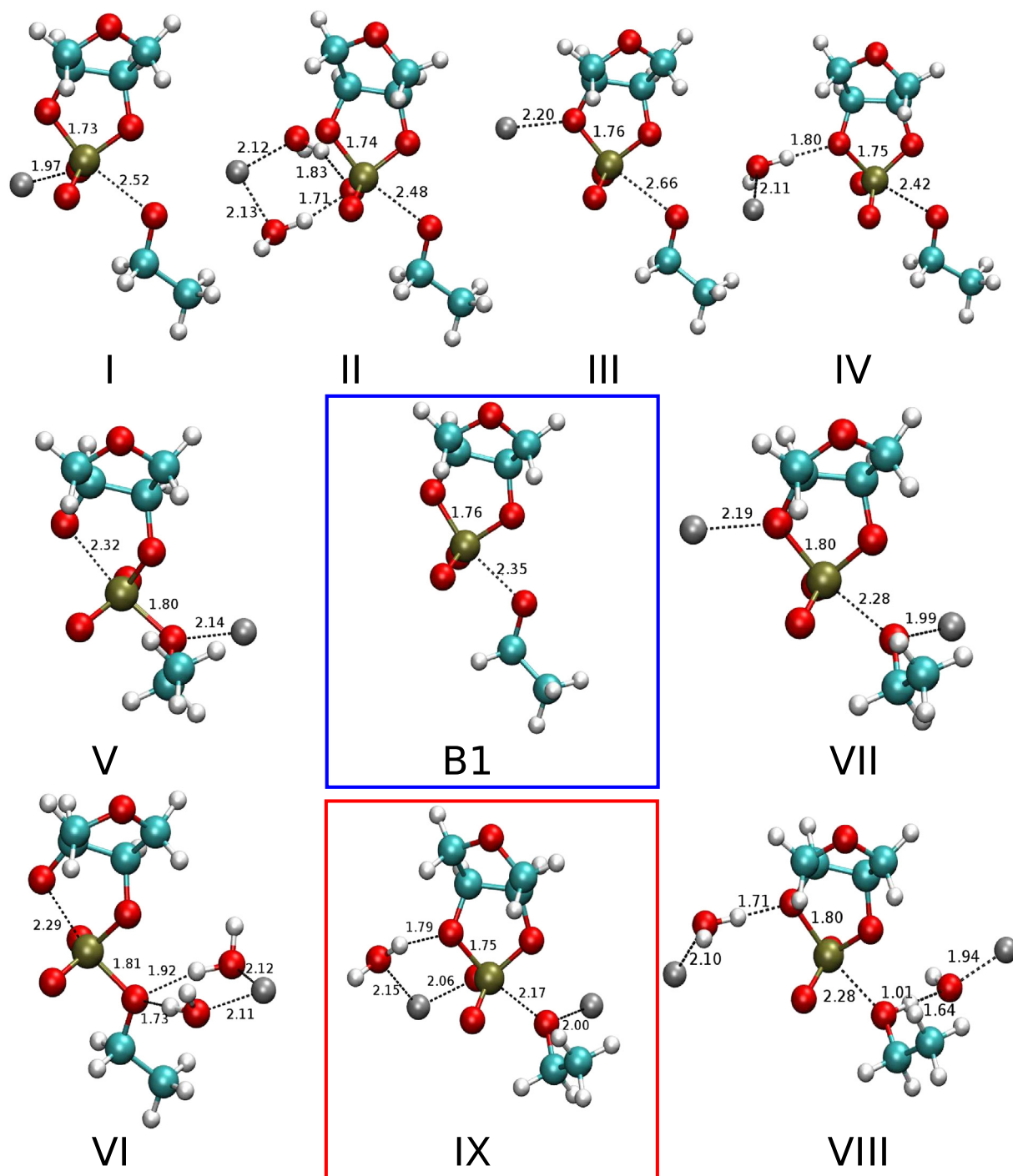


Fig. 2. TS structures located from all 9 Zn^{2+} binding models and comparison with the baseline model B1. Model IX matches best with experimental KIEs and has been highlighted. Key bond lengths in Å are labeled. All Zn^{2+} are saturated to hexacoordination by water but only key water molecules are shown for clarity.

2.3. Comparison between Zn^{2+} catalysis and enzyme catalysis

The transition state for RNA 2'-O-transphosphorylation catalyzed by RNase A exhibits a primary KIE signature, both from experiment and computation, that is very close to that produced upon Zn^{2+} binding (Table 1). This is evident by analyzing the normalized $k^{\text{Cat}}/k^{\text{BL}}$ values for the Zn^{2+} and RNase A transition states which are all within 1% of one another. The baseline normalized computational values are very close to the experimental values, but particularly striking is the internal

consistency for the $^{18}\text{k}_{\text{LG}}$ values between Zn^{2+} and RNase A system as determined from either theory or experiment. The most straight forward interpretation is that the Zn^{2+} ions produce a local TS bonding environment that is similar to that of the RNase A active site: one Zn^{2+} ion stabilizes the negatively charged reaction center in transition state similar to a protonated His12 in RNase A, while another Zn^{2+} ion enhances the leaving group departure analogous to the role of His19 (Fig. 3). This analysis sheds light on general principles involved in RNA catalysis.

Table 2

Comparison of calculated KIEs and reaction coordinate ξ values in the TSs from models I to IX.

Model	ξ (Å)	$^{18}k_{LG}$ (%D)	$^{18}k_{KNUC}$ (%D)	$^{18}k_{NPO}$ (%D)
B1	0.59	1.0416	1.0016	1.0029
Expt. w/o Zn	N/A	1.034(3)	0.997(1)	0.999(1)
I	0.79	1.0466 (2.3)	0.9986 (0.8)	1.0017 (−0.3)
II	0.74	1.0441 (2.1)	0.9986 (0.8)	1.0029 (−0.2)
III	0.90	1.0517 (2.8)	1.0040 (1.3)	1.0007 (−0.4)
IV	0.67	1.0417 (1.8)	1.0012 (1.1)	1.0031 (−0.2)
V	−0.53	1.0063 (−1.6)	1.0463 (5.6)	1.0015 (−0.3)
VI	−0.49	1.0051 (−1.7)	1.0484 (5.8)	1.0029 (−0.2)
VII	0.47	1.0324 (1.0)	1.0054 (1.5)	1.0017 (−0.3)
VIII	0.48	1.0080 (−1.4)	1.0079 (1.7)	1.0005 (−0.4)
IX	0.42	1.0276 (0.5)	0.9950 (0.4)	1.0028 (−0.2)
Expt. w. Zn	N/A	1.015(2)	0.986(4)	1.0007(2)

Model numbering is the same as in Fig. 1. Temperature is 90 °C for all calculations and experiment. Reaction coordinate ξ is defined as $\xi = R_2 - R_1$, where R_1 and R_2 are the P–O2' and P–O5' bond lengths, respectively. Percentage deviation %D is defined as $\%D = [(k^{cat}/k^{BL})_{Calc.} - (k^{cat}/k^{BL})_{Expt.}] \times 100\%$, where BL is the baseline model (B1) consistent with the series of Zn^{2+} calculations. The numbers in parentheses following the experimental values are the experimental uncertainties.

3. Conclusion

In conclusion, we explored the effect of different Zn^{2+} binding modes on the ^{18}O kinetic isotope effects for Zn^{2+} -catalyzed RNA 2'-O-transphosphorylation. Different Zn^{2+} binding modes yield distinct KIE signatures that can be connected to TS structure and bonding and used to aid in the interpretation of experimental measurements to give insight into mechanism. A unique binding mode was identified as being very closely aligned with recent experimental measurements. This mode involved two zinc ions, one directly coordinating the leaving group and the other directly coordinating a non-bridge phosphoryl oxygen while interacting with the nucleophile at solvent separation. This catalytic mode produces a KIE signature very close to that observed for the TS in RNase A, and leads to model TS structure that is also quite similar. We also identified the origin of the systematic overestimation of the $^{18}k_{LG}$ KIE value relative to experiment noted previously [15,19–21] which herein was shown to be corrected by inclusion of more realistic leaving group models. This work provides a predictive framework for the identification of Zn^{2+} ion binding modes in RNA 2'-O-transphosphorylation reactions from KIE measurements that will

advance our understanding of the role of divalent metal ions in mechanisms of RNA catalysis.

Computational methods

DFT calculations were performed using the B3LYP [24,25] functional which has been demonstrated to be reliable for zinc complexes [26]. The 6-31+G(d) basis set was used for H, C, N, O and P, while the SDD effective core potential [27] was applied to Zn. Solvation effects were treated with the polarizable continuum model [28] (PCM) using specialized atomic cavity radii for RNA catalysis adopted from previous work [15,19]. Water solvent with a dielectric constant of 78.4 is used in all PCM calculations. Kinetic isotope effects were calculated from the Bigeleisen equation [9] using the vibrational frequencies obtained from normal mode analysis of the optimized reactant and transition state geometries. All electronic structure calculations were carried out in Gaussian 09 package [29].

Transparency document

The Transparency document associated with this article can be found, in the online version.

Acknowledgments

The authors are grateful for financial support provided by the National Institutes of Health (GM062248 to D.M.Y., GM096000 to M.E.H. and AI081987 to J.A.P.). This work used the Extreme Science and Engineering Discovery Environment (XSEDE), which is supported by National Science Foundation grant number OCI-1053575.

References

- T.A. Steitz, J.A. Steitz, A general two-metal-ion mechanism for catalytic RNA, *Proc. Natl. Acad. Sci. U. S. A.* 90 (1993) 6498–6502.
- V.J. DeRose, Metal ion binding to catalytic RNA molecules, *Curr. Opin. Struct. Biol.* 13 (2003) 317–324.
- R.K.O. Sigel, A.M. Pyle, Alternative roles for metal ions in enzyme catalysis and the implications for ribozyme chemistry, *Chem. Rev.* 2007 (2007) 97–113.
- M. Forconi, D. Herschlag, Metal ion-based RNA cleavage as a structural probe, *Methods Enzymol.* 468 (2009) 91–106.

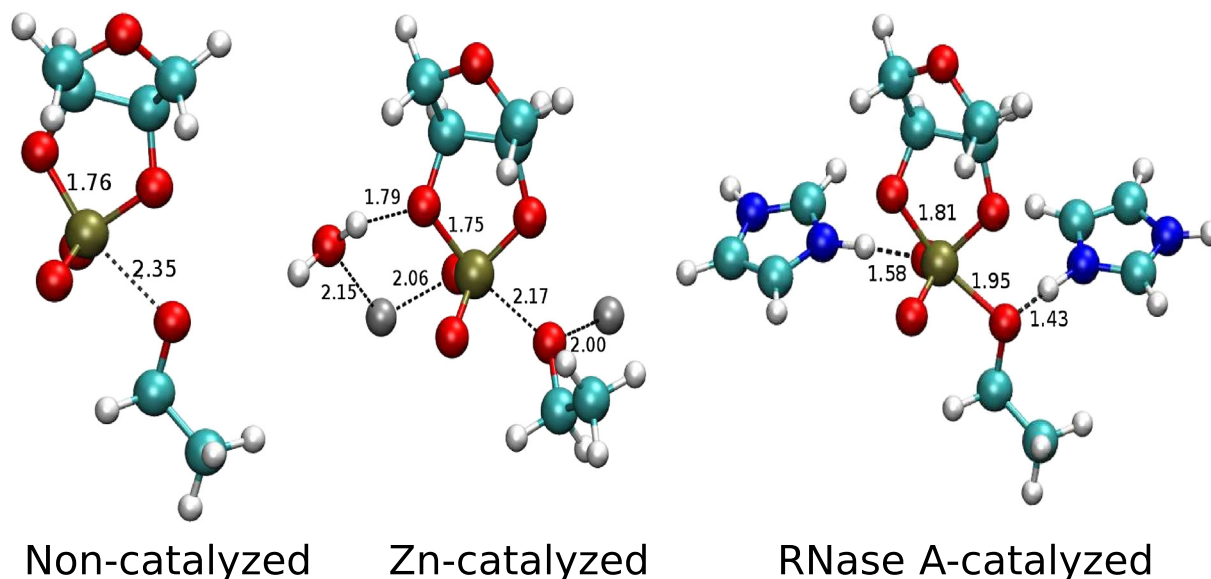


Fig. 3. Comparison of TS structures in baseline, Zn^{2+} -catalyzed and RNase A-catalyzed model reactions. The two imidazole rings in the RNase A model represents His12 (left) and His19 (right) residues in RNase A.

- [5] Z. Chval, D. Chvalova, F. Leclerc, Modeling the RNA 2'OH activation: possible roles of metal ion and nucleobase as catalysts in self-cleaving ribozymes, *J. Phys. Chem. B* 115 (2011) 10943–10956.
- [6] S.M. Fica, N. Tuttle, T. Novak, N.-S. Li, J. Lu, P. Koodathingal, Q. Dai, J.P. Staley, J.A. Piccirilli, RNA catalyses nuclear pre-mRNA splicing, *Nature* 503 (2013) 229–234.
- [7] W.L. Ward, K. Plakos, V.J. DeRose, Nucleic acid catalysis: metals, nucleobases, and other cofactors, *Chem. Rev.* 114 (2014) 4318–4342.
- [8] D.L. Kellerman, D.M. York, J.A. Piccirilli, M.E. Harris, Altered (transition) states: mechanisms of solution and enzyme catalyzed RNA 2'-O-transphosphorylation, *Curr. Opin. Chem. Biol.* 21 (2014) 96–102.
- [9] J. Bigeleisen, M. Wolfsberg, Theoretical and experimental aspects of isotope effects in chemical kinetics, *Adv. Chem. Phys.* 1 (1958) 15–76.
- [10] L.C.S. Melander, W.H. Saunders, *Reaction Rates of Isotopic Molecules*, Wiley, 1980.
- [11] A.C. Hengge, Isotope effects in the study of phosphoryl and sulfuryl transfer reactions, *Acc. Chem. Res.* 35 (2002) 105–112.
- [12] M. Wolfsberg, W.A. Van Hook, P. Paneth, *Isotope Effects in the Chemical, Geological and Bio Sciences*, Springer, 2009.
- [13] J.K. Lassila, J.G. Zalatan, D. Herschlag, Biological phosphoryl-transfer reactions: understanding mechanism and catalysis, *Annu. Rev. Biochem.* 80 (2011) 669–702.
- [14] K. Swiderek, P. Paneth, Binding isotope effects, *Chem. Rev.* 113 (2013) 7851–7879.
- [15] H. Gu, S. Zhang, K.-Y. Wong, B.K. Radak, T. Dissanayake, D.L. Kellerman, Q. Dai, M. Miyagi, V.E. Anderson, D.M. York, J.A. Piccirilli, M.E. Harris, Experimental and computational analysis of the transition state for ribonuclease A-catalyzed RNA 2'-O-transphosphorylation, *Proc. Natl. Acad. Sci. U. S. A.* 110 (2013) 13002–13007.
- [16] T. Humphry, S. Iyer, O. Iranzo, J.R. Morrow, J.P. Richard, P. Paneth, A.C. Hengge, Altered transition state for the reaction of an RNA model catalyzed by a dinuclear zinc(II) catalyst, *J. Am. Chem. Soc.* 130 (2008) 17858–17866.
- [17] H. Gao, Z. Ke, N. DeYonker, J. Wang, H. Xu, Z. Mao, D. Phillips, C. Zhao, Dinuclear Zn(II) complex catalyzed phosphodiester cleavage proceeds via a concerted mechanism: a density functional theory study, *J. Am. Chem. Soc.* 133 (2011) 2904–2915.
- [18] M.E. Harris, Q. Dai, H. Gu, D.L. Kellerman, J.A. Piccirilli, V.E. Anderson, Kinetic isotope effects for RNA cleavage by 2'-O-transphosphorylation: nucleophilic activation by specific base, *J. Am. Chem. Soc.* 132 (2010) 11613–11621.
- [19] K.-Y. Wong, H. Gu, S. Zhang, J.A. Piccirilli, M.E. Harris, D.M. York, Characterization of the reaction path and transition states for RNA transphosphorylation models from theory and experiment, *Angew. Chem. Int. Ed.* 51 (2012) 647–651.
- [20] H. Chen, T.J. Giese, M. Huang, K.-Y. Wong, M.E. Harris, D.M. York, Mechanistic insights into RNA transphosphorylation from kinetic isotope effects and linear free energy relationships of model reactions, *Chem. Eur. J.* 20 (2014) 14336–14343.
- [21] S. Zhang, H. Gu, H. Chen, E. Strong, D. Liang, Q. Dai, V.E. Anderson, J.A. Piccirilli, D.M. York, M.E. Harris, Experimental and Computational Analyses Reveal an Associative Transition State for Non-Enzymatic RNA 2'-O-transphosphorylation, 2015. (submitted for publication).
- [22] D.S. Wishart, et al., HMDB 3.0—the human metabolome database in 2013, *Nucleic Acids Res.* 41 (2013) 801–807.
- [23] P.F. Cook, *Enzyme Mechanism from Isotope Effects*, CRC Press, 1991.
- [24] A.D. Becke, Density-functional thermochemistry. III. The role of exact exchange, *J. Chem. Phys.* 98 (1993) 5648–5652.
- [25] C. Lee, W. Yang, R.G. Parr, Development of the Colle–Salvetti correlation energy formula into a functional of the electron density, *Phys. Rev. B* 37 (1988) 785–789.
- [26] U. Ryde, Carboxylate binding modes in zinc proteins: a theoretical study, *Biophys. J.* 77 (1999) 2777–2787.
- [27] M. Dolg, U. Wedig, H. Stoll, H. Preuss, Energy-adjusted ab initio pseudopotentials for the first row transition elements, *J. Chem. Phys.* 86 (1987) 866–872.
- [28] M. Cossi, N. Rega, G. Scalmani, V. Barone, Energies, structures, and electronic properties of molecules in solution with the C-PCM solvation model, *J. Comput. Chem.* 24 (2003) 669–681.
- [29] M.J. Frisch, et al., Gaussian 09, Revision A.02, Gaussian, Inc., Wallingford, CT, 2009.